Progress In Electromagnetics Research B, Vol. 4, 159–169, 2008

SCATTERING OF REFLECTOR ANTENNA WITH CONIC DIELECTRIC RADOME

O. I. Sukharevsky and V. A. Vasilets

Kharkiv University of Air Forces
77/79 Sumska Str., 61023, Kharkiv, Ukraine

Abstract—The calculation method for radar cross-section (RCS) of reflector antenna placed under cone-shape dielectric radome has been proposed. The method based on the integral representations for a desired scattering field with using Lorenz lemma. These integral equations considered electromagnetic interaction between an antenna screen and a radome. The analysis of RCS calculation results for model antenna system with a conic dielectric radome has been carried out.

1. INTRODUCTION

Most aerial targets (aircrafts, antiaircraft missiles with self-direction head) have sharpened bow radomes covered reflector antenna. This antenna system essentially increases the RCS level of the whole aerial object [1]. Thus, the creation of methods for calculation and RCS estimation obtaining of antenna systems with radome is very important for an aerial target detection. The investigation of scattering characteristics for antenna systems with radomes has been a subject of much fruitful study [2–13]. Intrasystem interactions springing up in illumination of the "antenna-radome" system lead to more complex calculations. The presence of electromagnetic interaction between antenna and radome can result to very appreciable changes (frequently, by resonance nature) of RCS of the whole antenna system and so RCS of the whole aerial object.

Proposed in [14] iterative method for "antenna-radome" system has been created in the following limiting conditions: All considerations carried out for two-dimensional models and the radome shape in principle have to weakly curved. In [15] the radome was replaced by a finite dielectric plate.

We propose the approximate method of RCS calculation for a three-dimensional reflector antenna with a conic dielectric radome.

This method takes into account single re-reflections between antenna and internal surface of radome.

2. MAIN CALCULATION RELATIONS

Let consider the model of a reflector antenna with a conic radome (Fig. 1). The incident plane electromagnetic wave is

$$\begin{aligned}\vec{E}^0(\vec{x}) &= \vec{p}^0 \exp\left(jk_0\left(\vec{R}^0\cdot\vec{x}\right)\right),\\ \vec{H}^0(\vec{x}) &= \sqrt{\frac{\varepsilon_0}{\mu_0}}\left(\vec{R}^0\times\vec{p}^0\right)\exp\left(jk_0\left(\vec{R}^0\cdot\vec{x}\right)\right).\end{aligned}\tag{1}$$

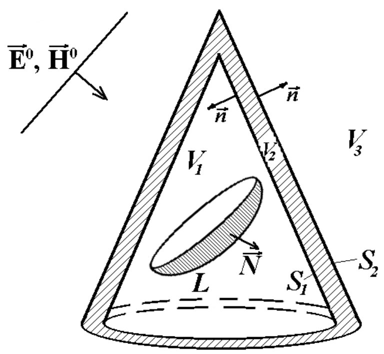

Figure 1. "Antenna-radome" system.

Let using the Lorenz lemma [16] for the desired full field $(\vec{E},\vec{H})$ and the auxiliary field $\left(\vec{\hat{E}},\vec{\hat{H}}\left(\vec{x}|\vec{x}_0,\vec{p}\right)\right)$, that is generated by a point electric dipole placed in point $\vec{x}_0$ with vector-moment $\vec{p}$ at the radome presence only. Then we obtain integral representation for a desired field

$$j\omega\vec{p}\cdot\vec{E}(\vec{x}_0) = j\omega\vec{p}\cdot\vec{E}_{rad}(\vec{x}_0) + \int_L \vec{\mathrm{K}}(\vec{x})\cdot\vec{\hat{E}}(\vec{x}|\,\vec{x}_0,\vec{p})ds. \tag{2}$$

Here $\vec{E}_{rad}(\vec{x}_0)$ is the field scattered by radome only, $\vec{\mathrm{K}}(x)$ is the current density at the antenna surface points. The integral term in (2) is the reflector L responses to the incident wave (1) with the account of electromagnetic interaction between a radome and an antenna. Let

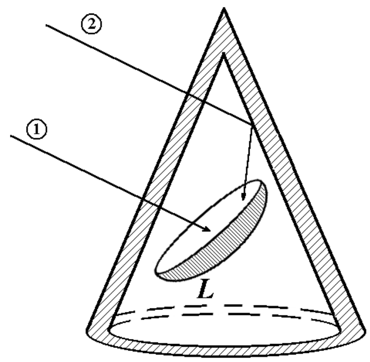

Figure 2. Advance of incident wave.

$\vec{x}_0 = -r\vec{R}^0$ and $r \to \infty$ we obtain the asymptotic expression for scattered field in far zone

$$\vec{p}\vec{E}(\vec{R}^0) \sim \vec{p}\vec{E}_{rad}(\vec{R}^0) - jk_0 \frac{e^{jk_0 r}}{4\pi r}\sqrt{\frac{\mu_0}{\varepsilon_0}} \int\limits_L \vec{\hat{E}}(\vec{x}) \cdot \vec{\mathrm{K}}(\vec{x}) ds. \qquad (3)$$

Here $\vec{\hat{E}}(\vec{x})$ is the field generated by the plane wave (1) at the antenna surface L points with the presence of single radome only. This field will be calculated using the geometrical optics approach. In this approach the field $\left(\vec{\hat{E}}(\vec{x}), \vec{\hat{H}}(\vec{x})\right)$ is represented as the sum of two fields. One of them reaches the antenna directly through illuminated radome surface (Fig. 2 — way 1), and the another field illuminates antenna after single re-reflection from the internal radome surface (Fig. 2 — way 2). So, the first term of this field can be written as

$$\vec{\hat{E}}_1(\vec{x}) = \left[\tau_\perp p_\perp \vec{e}_\perp + \tau_\| p_\| \left(\vec{R}^0 \times \vec{e}_\perp\right)\right] \exp\left(jk_0\left(\vec{R}^0 \cdot \vec{x}\right)\right) \qquad (4)$$

$$\vec{\hat{H}}_1(\vec{x}) = \sqrt{\frac{\varepsilon_0}{\mu_0}}\left[\tau_\perp p_\perp \left(\vec{R}^0 \times \vec{e}_\perp\right) - \tau_\| p_\| \vec{e}_\perp\right] \exp\left(jk_0\left(\vec{R}^0 \cdot \vec{x}\right)\right) \qquad (5)$$

where $\vec{e}_\perp = \frac{\vec{R}^0 \times \vec{n}}{\left|\vec{R}^0 \times \vec{n}\right|}$, $\vec{e}_\| = \left(\vec{R}^0 \times \vec{e}_\perp\right)$, $p_\perp = (\vec{p} \cdot \vec{e}_\perp)$, $p_\| = \left(\vec{p} \cdot \vec{e}_\|\right)$, $\vec{n}$ is a normal unit vector to a radome surface point.

The complex values $\tau_\perp$, $\tau_\|$ are the coefficients of plane electromagnetic wave that is passing through a parallel-sided layer tangent to radome (with radome parameters) for two mutually orthogonal polarizations. In case of $\|$ (parallel) polarization the electrical vector of the incident wave, vector $\vec{R}^0$ and the normal vector $\vec{n}$ at given point of radome surface are coplanar. For $\perp$ (perpendicular) polarization the electrical vector of incident wave is perpendicular both vectors $\vec{R}^0$ and $\vec{n}$. The general expression for passing coefficient can be presented in view

$$\tau = \left(\left(\cos\kappa\delta + \frac{j}{c}\sin\kappa\delta\right) + \left(\cos\kappa\delta - \frac{j}{c}\sin\kappa\delta\right)\rho\right)\exp\left(-jk_0\delta\cos\theta\right), \tag{6}$$

where ρ is the complex reflection coefficient for parallel-sided layer with radome parameters. It can be presented in view:

$$\rho = \frac{j\left(c^2-1\right)\sin\kappa\delta}{2c^2\cos\kappa\delta - j\left(c^2+1\right)\sin\kappa\delta}. \tag{7}$$

Here $c = \frac{\sqrt{\varepsilon' - \sin^2\theta}}{}\beta\cos\theta$, $\kappa = k_0\sqrt{\varepsilon' - \sin^2\theta}$, $\cos\theta = |(\vec{R}^0\cdot\vec{n})|$, $\sin^2\theta = 1 - (\vec{R}^0\cdot\vec{n})^2$, ε' is the relative permittivity of radome, δ is the radome thickness.

$$\beta = \begin{cases} 1 \text{ for } \perp \text{ polarization,} \\ \varepsilon' \text{ for } \parallel \text{ polarization.} \end{cases}$$

In the case of $\perp$ polarization $\rho = \rho_\perp$, $\tau = \tau_\perp$, and in the case of $\parallel$ polarization $\rho = \rho_\parallel$, $\tau = \tau_\parallel$.

If the beam, that passes radome in the some point $\vec{x}_0$, doesn't cross the antenna reflector, it have to cross the radome at another point $\vec{x}_1$. In this case the vector of electric intensity is

$$\vec{p}_1 = \tau_\perp p_\perp \vec{e}_\perp + \tau_\parallel p_\parallel \vec{e}_\parallel \tag{8}$$

for field that is falling on inside radome surface at point $\vec{x}_1$. The values $\tau_\perp$, $\tau_\parallel$, $\rho_\perp$, $\rho_\parallel$ in (8) obtained for point x_0. This vector $\vec{p}_1$ and relations (6), (7) can be used for obtaining $\tau_{1\perp}$, $\tau_{1\parallel}$, $\rho_{1\perp}$, $\rho_{1\parallel}$, $\vec{e}_{1\perp}$, $\vec{e}_{1\parallel}$. The expression for a field incidented on an antenna reflector L after the reflection from inside radome surface at point $\vec{x}_1$ (the way 2 on the Fig. 2) can be presented as

$$\begin{aligned} \vec{\hat{E}}_2(\vec{x}) &= \left[\rho_{1\perp}p_{1\perp}\vec{e}_{1\perp} + \rho_{1\parallel}p_{1\parallel}\left(\vec{R}_1\times\vec{e}_{1\perp}\right)\right] \\ &\quad \exp\left(jk_0\left[\left(\vec{R}^0\cdot\vec{x}_1\right) + \left(\vec{R}^1\cdot\vec{x}\right)\right]\right), \end{aligned} \tag{9}$$

$$\begin{aligned} \vec{\hat{H}}_2(\vec{x}) &= \sqrt{\frac{\varepsilon_0}{\mu_0}}\left[-\rho_{1\parallel}p_{1\parallel}\vec{e}_{1\perp} + \rho_{1\perp}p_{1\perp}\left(\vec{R}_1\times\vec{e}_{1\perp}\right)\right] \\ &\quad \exp\left(jk_0\left[\left(\vec{R}^0\cdot\vec{x}_1\right) + \left(\vec{R}^1\cdot\vec{x}\right)\right]\right), \end{aligned} \tag{10}$$

where $\vec{R}^1 = \vec{R}^0 - 2\vec{n}(\vec{x}_1)\left(\vec{R}^0 \cdot \vec{n}(\vec{x}_1)\right)$.

The current density $\vec{\mathrm{K}}(\vec{x})$ on the antenna surface is calculated as a sum of currents generated by fields of "direct" and "re-reflection" waves (Fig. 2) on the antenna surface. In the physical optics approach the current density can be represented as

$$\vec{\mathrm{K}}(\vec{x}) = 2\left(\vec{N} \times \vec{\tilde{H}}\right) \tag{11}$$

where $\vec{N}$ is a normal unit vector to antenna surface, and $\vec{\tilde{H}}$ can be calculated as sum of magnetic-field strengthens for first and second ways (Fig. 2) of a wave propagation in the accordance with expressions (5) and (10). The field $\vec{p}\vec{E}_{rad}(\vec{R}^0)$ scattered by radome can be calculated in Kirchhoff approach

$$\begin{aligned}\vec{p}\vec{E}_{rad}(\vec{R}^0) \approx -jk_0\frac{e^{jk_0r}}{4\pi r} \times \iint\limits_{S_{ill}} \left[\left(\vec{p} \cdot \left(\vec{n} \times \vec{H}'(\vec{x})\right)\right)\sqrt{\frac{\mu_0}{\varepsilon_0}}\right. \\ \left. +\vec{E}'(\vec{x}) \cdot \left(\vec{n} \times \left(\vec{p} \times \vec{R}^0\right)\right)\right] \exp\left(jk_0\left(\vec{R}^0 \cdot \vec{x}\right)\right) ds. \end{aligned} \tag{12}$$

Here $\left(\vec{E}', \vec{H}'\right)$ is the field near illuminated radome surface S_{ill}, that can be estimated using Kirchhoff approach

$$\begin{aligned}\vec{E}'(\vec{x}) &\approx \left[\rho_\perp(\vec{x})p_\perp(\vec{x})\frac{\left(\vec{R}^1 \times \vec{n}\right)}{\left|\vec{R}^1 \times \vec{n}\right|} + \rho_\parallel(\vec{x})p_\parallel(\vec{x})\frac{\vec{R}^1 \times \left(\vec{R}^1 \times \vec{n}\right)}{\left|\vec{R}^1 \times \left(\vec{R}^1 \times \vec{n}\right)\right|}\right] \\ &\quad \exp\left(jk_0\left(\vec{R}^1 \cdot \vec{x}\right)\right), \end{aligned} \tag{13}$$

$$\vec{H}'(\vec{x}) = \frac{1}{j\omega\mu_0}\vec{\nabla} \times \vec{E}'(\vec{x}), \tag{14}$$

where $\vec{R}^1 = \vec{R}^0 - 2\vec{n}\left(\vec{R}^0 \cdot \vec{n}\right)$. $\vec{n} = \vec{n}(x)$ is the normal vector to the outside radome surface S_2. The expression (12) for conic radome can be transformed to single integral over angle α concerned with the illuminated radome surface:

$$\vec{p} \cdot \vec{E}_{rad}\left(\vec{R}^0\right) \approx -jk_0\frac{e^{jk_0r}}{4\pi r}\frac{\sin\theta}{\cos^2\gamma}\int\limits_{\alpha_0}^{\alpha_1}\Psi(\alpha)d\alpha, \tag{15}$$

where

$$\Psi(\alpha) = F(\alpha)\left[\frac{h\exp\left(j2k_0h\varphi(\alpha)\right)}{2jk_0\varphi(\alpha)} + \frac{\exp\left(j2k_0h\varphi(\alpha)\right) - 1}{4k_0^2\varphi^2(\alpha)}\right],$$

$$F(\alpha) = \left(\rho_{\perp}(\alpha)\, p_{\perp}^2(\alpha) - \rho_{\parallel}(\alpha)\, p_{\parallel}^2(\alpha)\right)\left(\vec{R}^0 \cdot \vec{n}(\alpha)\right),$$

$$\varphi(\alpha) = tg\theta\left(R_1^0 \cos\alpha + R_2^0 \sin\alpha\right) + R_3^0,$$

$$\alpha_0 = \operatorname{arcctg}\frac{\eta}{\sqrt{1-\eta^2}}, \quad \alpha_1 = 2\pi - \alpha_0, \quad \eta = \frac{tg\theta}{tg\gamma}.$$

Here h is the radome height, θ is the half-angle of radome cone, γ is the angle between radome axis and vector, $\vec{n}(\alpha)$ is the normal vector to outside radome surface S_2.

3. CALCULATION RESULTS

Figure 3 illustrates the geometry of the calculation model. The vertex of the radome cone is placed at the point of origin and cone axis coincide with axis Oz. The radome height is $h = 1$ m, half-angle is $\theta = 20°$, relative permittivity of radome material $\varepsilon' = 7$. The distance between the cone vertex and the antenna center point is $d = 0.75$ m, the antenna radius $a = 0.25$ m. Antenna can turn around axis Oy. The unit vector of the incident wave direction $\vec{R}^0$ is placed in plane $Oxz(\vec{R}^0 = \{\sin\gamma, 0, \cos\gamma\})$.

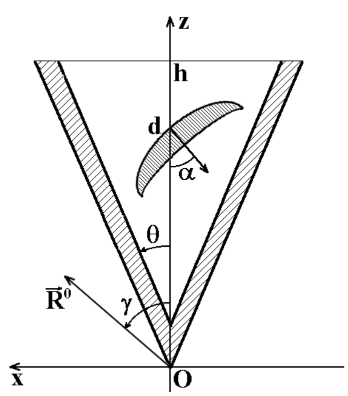

Figure 3. Geometry of the antenna calculation model.

The three antenna shapes have been considered — with almost plane surface (focal parameter is $q = 10$ m reflector depth is near 3 mm), antenna with focal parameter $q = 1$ m, (reflector depth is near

3 sm) and "deep" antenna (focal parameter is $q = 25$ sm, reflector depth is near 12 sm).

RCS dependence from the illumination angle γ for antenna without radome is shown in Fig. 4. The antenna focal parameter is $q = 1$ m, wave-length is $\lambda = 3$ sm. The angle $\alpha = 45°$. RCS dependence for antenna at the presence of radome is shown in Fig. 5. The radome thickness is 5.6 mm and matched for hade angle 20°. The polarization vector of incident wave is normal to Oxz (u-polarization). The gray curve illustrates the contribution of "direct" wave (Fig. 2 — way1), dash curve-the contribution of "re-reflection" wave (Fig. 2 — way2), a solid black line is the whole antenna RCS. The RCS of "antenna-radome" system is shown in Fig. 6. The thin solid black line illustrates the antenna RCS, dash gray curve — the contribution of radome, thick black line is the RCS of system "antenna-radome". The analysis of Figs. 5, 6 and their comparison with RCS of antenna without radome shows that matched radome changes RCS faintly for wide range of illumination angels. However for some illumination angles the accounting of radome effect changes RCS essentially. So, for $\gamma = 45°$ (antenna illuminates along its axis) the radome presence reduces antenna RCS and "antenna-radome" system RCS in 7 times. The accounting of "re-reflection" wave (Fig. 2 — way2) essentially changes RCS for $\gamma > 60°$. The reflection from radome gives the essential effect for small angles γ and for $\gamma \cong 70°$ when the vector of the incident wave direction $\vec{R}^0$ is normal to radome generatrix.

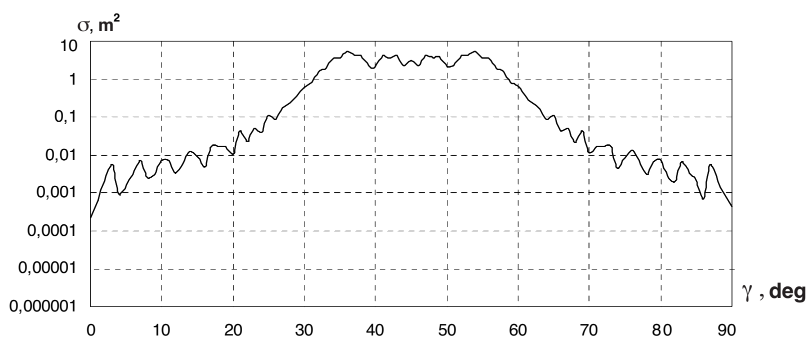

Figure 4. RCS of antenna without radome.

The RCS dependencies for case when the polarization vector is parallel to Oxz (v-polarization) have been presented in Figs. 7 and 8.

The radome effect for "antenna-radome" system RCS is reduced in the case of v-polarization. This fact is expressed in reducing of "re-reflection" wave contribution, in reducing of radome reflection and in

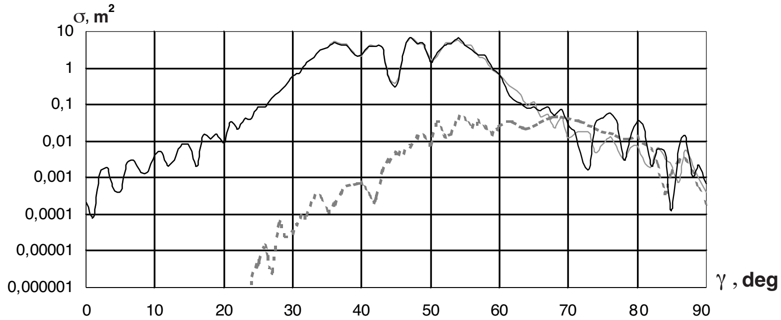

Figure 5. RCS of antenna at the presence of radome (u-polarization).

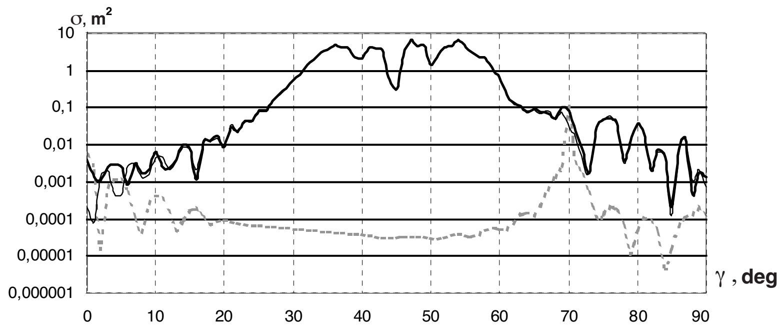

Figure 6. RCS of "antenna-radome" system (u-polarization).

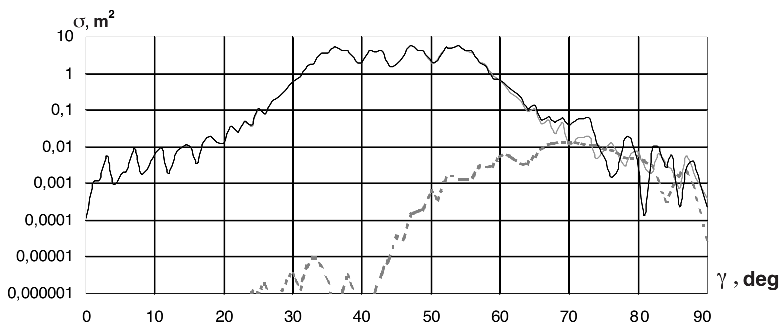

Figure 7. RCS of antenna at the presence of radome (v-polarization).

the general behavior of system RCS: In the case of v-polarization. The RCS of "antenna-radome" system is closer to RCS of antenna without radome than in the case of u-polarization. So, for $\gamma = 45°$ system RCS

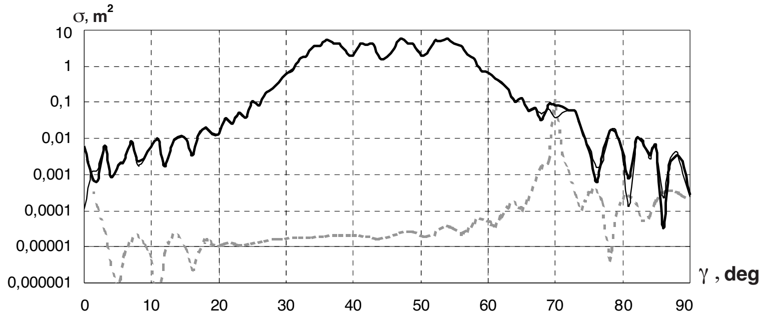

Figure 8. RCS for "antenna-radome" system (v-polarization).

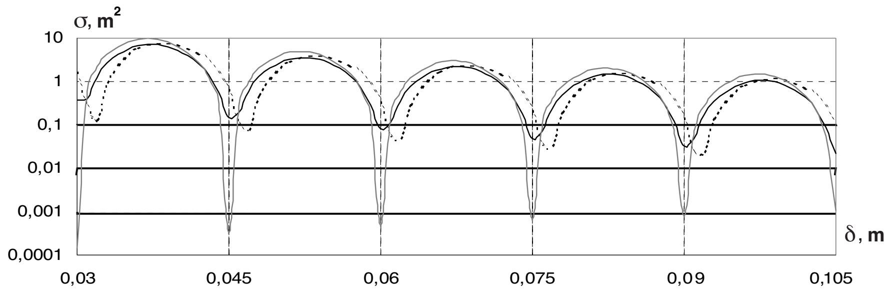

Figure 9. Antenna RCS dependency from it depth.

in case of v-polarization doesn't differ practically from RCS of antenna without radome.

Let consider RCS dependencies from antenna depth for axial incidence (Fig. 9). Reflector depth δ is changed from 3 sm (one sounding wave length) to 10.5 sm (3.5 wave lengths). The focal parameter is changed from $q = 1$ m to $q = 0.3$ m. Thin gray line (Fig. 9) indicates the antenna RCS dependency from its depth in the case of radome absence. The solid black line indicates RCS of "antenna-radome" system for v-polarization, the dash black line indicates RCS of "antenna-radome" system for u-polarization.

The RCS dependencies at the presence of radome moves right relatively RCS dependence for single antenna. The Fresnel zones are formed on the parabolic antenna surface. For axial incidence RCS depends on composition of fields scattered by the first and the last Fresnel zones on antenna surface. The change of reflector depth leads to appearance or disappearance of Fresnel zones near the antenna edge. Accordingly, periodicity of RCS changes are connected with incident wave length value.

The analysis of calculation results for RCS of system with plane reflector ($q = 10$ m) shows the same tendencies as for antenna with $q = 1$ m — the essential contribution of reflection from radome and "re-reflection" wave to whole scattered field for some illumination angles. The RCS for system with "deep" antenna ($q = 0.25$ m) changes from 1 to 10 m^2 for any sounding angle γ (from 0 to 90°). In this case the effect of "re-reflection" doesn't change practically the antenna RCS.

4. CONCLUSION

The accounting of electromagnetic interactions between an antenna and a radome allows to increase the calculation accuracy for antenna system RCS and for RCS of objects with "antenna-radome" system. The RCS dependencies from illumination angles and another factors are quickly oscillating and wide-range changing. Thus it is need to average RCS values in corresponding ranges for obtaining stable values of "antenna-radome" system RCS of aerial objects.

REFERENCES

1. Ruck, G. T. (ed.), *Antenna Scattering Radar Cross Section Handbook*, Vol. 2, N.Y., 1970.
2. Oğuzer, T. and A. Altintas, "Free content analysis of the nonconcentric reflector antenna-in-radome system by the iterative reflector antenna and radome interaction," *Journal of Electromagnetic Waves and Applications*, Vol. 21, No. 1, 57–70, 2007.
3. Gustafsson, M., "RCS reduction of integrated antenna arrays with resistive sheets," *Journal of Electromagnetic Waves and Applications*, Vol. 20, No. 1, 27–40, 2006.
4. Nie, X. C., Y. B. Gan, N. Yuan, C. F. Wang, and L. W. Li, "An efficient hybrid method for analysis of slot arrays enclosed by a large radome," *Journal of Electromagnetic Waves and Applications*, Vol. 20, No. 2, 249–264, 2006.
5. Oğuzer, T. and A. Altintas, "Analysis of the nonconcentric radome-enclosed cylindrical reflector antenna system, e-polarization case," *Journal of Electromagnetic Waves and Applications*, Vol. 19, No. 15, 2093–2111, 2005.
6. Oğuzer, T., "Analysis of a cylindrical reflector antenna encased in a concentric dielectric radome with a resistive or pec inner circular grating," *Journal of Electromagnetic Waves and Applications*, Vol. 16, No. 4, 493–513, 2002.

7. Nie, X. C., N. Yuan, L. W. Li, T. S. Yeo, and Y. B. Gan, "Fast analysis of electromagnetic transmission through arbitrarily shaped radome using precorrected-FFT method," *Progress In Electromagnetics Research*, PIER 54, 37–59, 2005.
8. Guo, J., J.-Y. Li, and Q.-Z. Liu, "Analysis of antenna array with arbitrary shaped radomes using fast algorithm based on VSIE," *Journal of Electromagnetic Waves and Applications*, Vol. 20, No. 10, 1399–1410, 2006.
9. Zou, Y., J.-Y. Li, and Q.-Z. Liu, "Modified mode decomposition for analyzing antennas with body of revolution radome," *Journal of Electromagnetic Waves and Applications*, Vol. 21, No. 10, 1403–1410, 2007.
10. Zou, Y., Q.-Z. Liu, and J. Guo, "Fast analysis of body of revolution radomes with method of moments," *Journal of Electromagnetic Waves and Applications*, Vol. 21, No. 13, 1803–1817, 2007.
11. Hemon, R., P. Pouliguen, H. He, J. Saillard, and J.-F. Damiens, "Computation of EM field scattered by an open-ended cavity and by a cavity under radome using the iterative physical optics," *Progress In Electromagnetics Research*, PIER 80, 37–59, 2008.
12. Leong, M. S., L. W. Li, X. Ma, P. S. Kooi, and T. S. Yeo, "Analysis of radiation characteristics of an open circular waveguide asymmetrically covered by a dielectric layered hemi-spherical radome," *Progress In Electromagnetics Research*, PIER 34, 253–270, 2001.
13. Li, L. W., L. Zhou, M. S. Leong, T. S. Yeo, and P. S. Kooi, "An open-ended circular waveguide with an infinite conducting flange covered by a dielectric hemi-spherical radome shell: Full-wave analysis and green dyadics," *Progress In Electromagnetics Research*, PIER 21, 221–245, 1999.
14. Mikhailov, G. D., S. N. Kutischev, and O. E. Kir'yanov, "Radar cross-section of reflector antenna with dielectric radome," *Izvestiya Vuzov. Radiofizika*, Vol. XLII, No. 9, 879–885, 1999 (in Russian).
15. Zamyatin, V. I. and O. I. Sukharevsky, "Backscattering of exterior source waves by reflector antenna with dielectric envelope," *Anntenny*, Vol. 37, 78–87, Radio i svyaz, Moscow, 1990 (in Russian).
16. Silver, S., *Microwave Antenna Theory and Design*, MIT Series, Vol. 12, McGraw Hill, 1949.